LES of Premixed V-Flame Using Anisotropic SGS Scalar Flux Model

P. Pantangi[1], M. Chirgui[1], F. Dinkelacker[2], A. Sadiki[1]
pantangi@ekt.tu-darmstadt.de
[1]Darmstadt University of Technology, Department. of Mechanical Engineering, Energy and powerplant technology, Petersenstr. 30, 64287 Darmstat, Germany.
[2]Leibniz University of Hannover, Institute of Technical Combustion, Welfengarten 1a, 30167 Hannover, Germany

Abstract

The present paper describes the evaluation of the newly developed Sub Grid Scale(SGS) scalar flux models on rod stabilized premixed methane V-flame. LES simulations are performed with the dynamic Smagorinsky SGS model for the flow field. The SGS scalar flux has been modelled by the recently proposed Eddy diffusivity, Anisotropic model together with using dynamic coefficients. In this work combustion is modelled by flamelet generated manifold (FGM)-tabulated chemistry approach, in which a variable local equivalence ratio due to a possible entrainment of the environment air is included through a mixture fraction variable, is integrated into an appropriate complete model. To assess the model capability, LES results of the rod stabilized flame are compared against experimental data. A satisfactory agreement for the flow field quantities and species concentrations is achieved along with an assessment of the SGS scalar fluxes.

Introduction

Turbulent premixed combustion plays an important role in many technical applications, e.g., in spark ignition engines and in gas turbines. While RANS computations of premixed flames are well reported in the literature, LES of premixed combustion remains difficult due to the thickness of the premixed flame about 0.1–1 mm and generally smaller than the LES mesh size. Physical and chemical features of combustion LES have been discussed by Janicka and Sadik [1], and Pitsch [2] with emphasis focused on important aspects of an overall model. Several approaches have been reviewed for modeling of premixed turbulent combustion; this comprehends turbulence controlled models (eddy break up, eddy dissipation models), statistical approach based models (PDF Transport equations, CMC, etc.), flamelet based models (surface Density models, G-equations, BML based models) or artificially thickened flame (ATF) approach. With regard to chemistry, the detail of chemistry is unavoidable if one has to address auto-ignition, flame stabilization, recirculating products which may include intermediate species, and the prediction of some pollutants [3,4,5]. The reduction and tabulation of chemical species behaviour prior to LES remains one of the available options that is being investigated to downsize combustion chemistry in order to make it compatible with flow solvers.

Efforts to extend the applicability of LES technique to premixed turbulent flame description are pursued here. To account for kinetic effects and flame stabilization in this work, the flamelet generated manifolds (FGM) method is introduced [5,6] and coupled to LES. This is achieved by incorporating into the CFD an additional transport equation for the progress

variable besides the mixture fraction equation and the classical flow governing equations. The resulting complete model is applied to simulate a laboratory-scale turbulent V-flame for which comprehensive experimental data are available.

A V-shape flame is generated when a premixed flame is stabilized on a hot wire or a rod [7] . In a laminar flow environment, the reaction layer propagates against the incoming fluid and a premixed V-shape flame is built. In the case of a turbulent flow, the two wings of the flame are wrinkled by velocity fluctuations and the V-flame is obtained in mean (see Fig.1). As pointed out by Domingo et al. [8] the flame stabilized by the rod takes benefit from the recirculation of hot products behind the obstacle, while the flame stabilized on a hot wire is initiated by the energy released by the wire. Thereby the very localized burning kernel serves to stabilize a premixed flame that develops downstream. Besides 2D DNS [8] and 3D DNS [9] calculations for low Reynolds number configurations, LES of V-flame are very rare. Manickam et al. [10] applied an algebraic flame surface wrinkling model to study rod stabilized flames. They compared the performance of a RNG k-Epsilon RANS model and a standard Smagorinsky LES using the commercial code Fluent to address the flow past the cylinder along with effects such as vortex shedding, lift and drag forces. To meet the need for reliable predictive method to aid mixing safety studies and the design/optimization of practical high Reynolds number mixing and combustion systems, it is essential that turbulent SGS models for scalar in CFD be able to address accurately major effects at low computational cost. Hence Huai et al. [5,7] reported LES results in which an adequate model for the SGS scalar flux vector has been applied. This methodology was validated in different configurations of various complexity involving gaseous and liquid non-reacting flows, respectively [21,23,24]. Here, an advanced SGS scalar model package is presented to develop Large Eddy Simulation (LES) of turbulent reactive flows. In the present work focus is put on the prediction of the overall flow field, combustion and the assessment of the SGS scalar flux model is carried out.

After introducing the numerical procedure and the modelling technique employed for the present work, following section provides comparisons between experimental and simulation results and discussions. The last section is devoted to conclusions.

Numerical Procedure and Modelling Technique

In this paper, a classical approach for LES is used. To separate the large from small-scale structures in LES, filtering operations are applied to the governing equations, which are the momentum equation (2) along with the continuity equation (1) used to describe the motion of low Mach number Newtonian fluids. In addition, the change of mixture fraction, ξ, caused by the turbulent convection and diffusion of a passive (or conserved) scalar is given by the transport equation (3).

$$\frac{\partial \breve{\rho}}{\partial t} + \frac{\partial \breve{\rho} \overline{u}_i}{\partial x_i} = 0 \tag{1}$$

$$\frac{\partial}{\partial t}(\breve{\rho}\overline{u}_i) + \frac{\partial}{\partial x_j}(\breve{\rho}\overline{u}_i\overline{u}_j) = \frac{\partial}{\partial x_j}\left[\breve{\rho}\breve{\nu}\left(\frac{\partial \overline{u}_i}{\partial x_j} + \frac{\partial \overline{u}_j}{\partial x_i}\right) - \frac{2}{3}\breve{\rho}\breve{\nu}\frac{\partial \overline{u}_k}{\partial x_k}\delta_{ij} - \breve{\rho}\tau_{ij}^{sgs}\right] - \frac{\partial \overline{p}}{\partial x_i} + \breve{\rho} g_i \tag{2}$$

$$\frac{\partial}{\partial t}\breve{\rho}\bar{\xi}+\frac{\partial}{\partial x_i}\left(\breve{\rho}\bar{u}_i\bar{\xi}\right)=\frac{\partial}{\partial x_i}\left(\breve{\rho}\bar{D}_f\frac{\partial\bar{\xi}}{\partial x_i}\right)-\frac{\partial}{\partial x_i}\left(\breve{\rho}J_i^{sgs}\right) \tag{3}$$

In equations (1)-(3) the quantity u_i (i=1, 2, 3) denotes the velocity components at x_i direction, ρ the density, p the hydrostatic pressure and δ_{ij} the Kronecker delta. The quantity ν is the molecular viscosity and D_f the molecular diffusivity coefficient.

To take into account chemical kinetic effects, the introduction of variables to track reaction progress is useful. This is achieved by incorporating into the CFD, besides the mixture fraction equation already available, an additional transport equation for the reaction progress variable (RPV):

$$\frac{\partial}{\partial t}\breve{\rho}\bar{Y}_\alpha+\frac{\partial}{\partial x_i}\left(\breve{\rho}\bar{u}_i\bar{Y}_\alpha\right)=\frac{\partial}{\partial x_i}\left(\breve{\rho}D\frac{\partial\bar{Y}_\alpha}{\partial x_i}\right)-\frac{\partial}{\partial x_i}\left(\breve{\rho}J_i^{sgs}\right)+\bar{S}_\alpha,\ \alpha=\{1,2,...\} \tag{4}$$

where $\bar{Y}_\alpha$ is the filtered concentration of the reaction progress variable α. The quantity D denotes the molecular diffusivity coefficient. For the combustion process under investigation the Y_α has been defined as

$$Y_\alpha\equiv Y_{RPV}=\frac{Y_{CO_2}}{M_{CO_2}} \tag{4b}$$

where M_i denoted the molar mass of the species i. The equations (1)-(4) govern the evolution of the large, energy-carrying, scales of flow and mixing field denoted by an over-bar. In flow and scalar field, the effect of the small scales appears through the SGS stress tensor and the SGS scalar flux vector,

$$\tau_{ij}^{SGS}=\overline{u_iu_j}-\bar{u}_i\bar{u}_j \tag{5}$$

$$J_i^{sgs}=\overline{u_iz_\alpha}-\bar{u}_i\bar{z}_\alpha,\quad z\equiv(\xi,Y_\alpha) \tag{6}$$

respectively. The last term, $\bar{S}_\alpha$, in equation (4) is the filtered chemical reaction rate. Together with the quantities (5) and (6) it must be modelled in order to obtain a closed system of equations (1) - (4).

A Smagorinsky-model with dynamic procedure according to Germano et al. [11] is applied to determine the subgrid scale stresses. In order to stabilize the model, the modification proposed by Sagaut [12] is applied. In addition a clipping approach will reset negative Germano coefficient C_s to zero to avoid destabilizing values of the model coefficient. No special wall-treatment is included in the subgrid-scale model. We rather rely on the ability of the dynamic procedure to capture the correct asymptotic behaviour of the turbulent flow when approaching the wall (see e.g. Wegner et al., [13]). A detailed discussion of this issue is reported by Wegner [14]. Here three different formulations for modelling the sub-grid scale

scalar flux for the mixture fraction and in the RPV equations are proposed for investigation. First one is a classical gradient ansatz (7) using a constant turbulent Schmidt number of 0.7.

$$J_i^{sgs} = -\frac{\upsilon_t}{\sigma_t}\frac{\partial \overline{z}}{\partial x_i} \quad \upsilon_t = C_s \Delta^2 \left|\overline{S}\right| \tag{7}$$

υ_t is turbulent viscosity, σ_t is turbulent Schmidt number and $\left|\overline{S}\right|$ is the absolute values of strain rate. Second formulation of scalar flux is based on modelling of coefficient υ_t / σ_t in equation (7) dynamically(Dynamic EDM) as detailed by Cabot [22].

Third formulation of SGS scalar flux model in this work is expressed as an explicit anisotropy-resolving algebraic model derived from the transport equation of the SGS scalar flux vector, such that the irreversibility requirements of the second law of thermodynamics are automatically fulfilled by the suggested parameterization [24]. In its at least cubic form, the chosen new model combines the conventional linear eddy diffusivity model(EDM) with two additional terms. The first term involves the gradient of the filtered scalar field in cubic form and the second couples the (deviatoric) SGS stress tensor and the gradient of the filtered scalar field [21]. Here we restrict ourselves to linear terms in scalar gradient. The simplest model case thus reduces to

$$J_i^{SGS} = -D_{ed}\frac{\partial \overline{Z}}{\partial x_i} + D_{dev} T_{SGS} \tau_{ij}^{SGS(dev)} \frac{\partial \overline{Z}}{\partial x_j} \tag{8}$$

where $D_{(\cdot)}$ are the model coefficients. This model involves a tensor of diffusivity

$$D_{ij}^{SGS} = -D_{ed}\delta_{ij} + D_{dev} T_{SGS} \tau_{ij}^{SGS(dev)} \tag{9}$$

According to the modeling level used for the deviatoric part of the SGS stress tensor (linear, non-linear, and anisotropic) this model may lead to various special models that have been proposed in the literature. A detailed analysis of this consideration can be found in Sadiki et al., [21]. Restricted ourselves in this paper to Smagorinsky type model and to linear terms in scalar gradient in eq. (8), the simplest model case to be considered can be derived by expressing the SGS time scale in (8) in terms of the filter size and the SGS viscosity defined in the Smagorinsky model. Equation (8) then reduces to

$$J_i^{SGS} = -D_{ed}\frac{\partial \overline{Z}}{\partial x_i} + D_{an}\Delta^2 \overline{S}_{ij}\frac{\partial \overline{Z}}{\partial x_j} = D_{ij}^{Smag}\frac{\partial \overline{Z}}{\partial x_j}; \tag{10}$$

$$D_{ij}^{Smag} = -D_{ed}\delta_{ij} + D_{an}\Delta^2 \overline{S}_{ij} \tag{11}$$

where D_i^{Smag} is the reduced eddy diffusivity tensor. In particular

$$\sigma_t = [\mathrm{Sc}_t, \mathrm{Pr}] \quad , \mathrm{D}_{ed} = \frac{\upsilon_t}{\sigma_t} \tag{12}$$

expresses the well known Eddy diffusivity coefficient. All the model parameters in (3) or (5, 6) have to be determined dynamically according to the requirements along the entropy inequality treatment [21]. The SGS scalar flux model (10, 11) has been successfully validated in different configurations along with a jet in cross flow as experimentally investigated by Andreapoulos[26], a mixing layer without chemical reactions [25] and a jet in channel water flow by Meyer [12]. For details, see Huai [15, 23, 25]. Here focus is put on the ability of the

new models to well capture the SGS flux in combustion environments based on their proved performance in both reactive and non-reactive high Schmidt number liquid flows.

The remaining term to be closed, the chemical reaction term, is modelled following the FGM method. As any flamelet based model, flamelet generated manifolds are based on the idea that a multi- dimensional flame can be represented by a set of one-dimensional flamelets. The method is therefore based on the laminar flamelet equations and includes ILDM reduction methodology by solving transport equations for a given number of progress variables. However, instead of considering diffusion flamelets, the FGM's used are based on steady 1-D premixed flames. In the frame of this work one reaction progress variable as defined in equation (4b) has been used. In the following it is labelled $Y_1 \equiv y$. Dealing with an unconfined configuration, the entrainment of the environment air is possible and may lead to a variable local equivalence ratio. This is taken into account by introducing a mixture fraction variable as described in (3).

According to this approach a Favre-filtered thermo-chemical quantity, ϕ, is calculated by integrating over the joint PDF of mixture fraction and the RPV while accounting for the turbulence-chemistry interaction.

$$\tilde{\phi} = \int_0^1 \int_0^1 \phi(\xi, y^*) P(\xi, y^*) dy^* d\xi \tag{13}$$

In eq. (13), (*) expresses a normalized quantity by its value at chemical equilibrium and the instantaneous thermo-chemical quantities are provided in a detailed chemistry table. Details about this procedure can be found in Wegner [14].

Since the reaction progress variable is statistically independent from the mixture composition, the unknown PDF can be split up as a product of two single-variable PDF's, the mixture fraction and the progress variable, respectively. Each one-variable PDF is then assumed to have a presumed form. For mixture fraction, we employ the Beta-form determined by the filtered mean value and the variance, whilst a delta-function only determined by the filtered mean of the RPV is chosen for the RPV as a first-order approximation in the context of the present work.

$$P(\xi, y^*) = P(\xi) \bullet P(y^*) \tag{14}$$

$$P(\xi, y^*) = \beta(\xi; \tilde{\xi}, \widetilde{\xi''^2}) \bullet \delta(\widetilde{y^*}) = P(\xi; \tilde{\xi}, \widetilde{\xi''^2}, \widetilde{y^*}) \tag{15}$$

A discussion of this issue is reported in Landenfeld et al. [16]. According to (15) the thermo-chemical quantities can then be parameterized and tabulated in the so-called pre-integrated tables (tabulated SGS chemical parameters) as function of the filtered mixture fraction, its variance and the normalized filtered RPV:

$$\tilde{\phi} = f(\tilde{\xi}, \widetilde{\xi''^2}, \widetilde{y^*}) \tag{16}$$

Thereby the mixture fraction variance is obtained according to the simple gradient formulation

$$\widetilde{\xi''^2} \approx C_{eq} \Delta^2 \frac{\partial^2 \tilde{\xi}}{\partial x_i^2} \qquad (17)$$

In (17) the model coefficient Ceq is set to 0.15 in the present work. The source terms of RPV from the pre-integrated premixed FGM table for methane-air combustion at 1 bar are presented in Figure 1. Flammability limit of the methane air premixed combustion in mixture fraction space extents from 0.01 to 0.02 and in normalized progress variable space it is from 0.4 to 0.95. To capture well this narrow flammability zone well, the FGM table is constructed using 901 mixture fraction nodes [20].

Configuration and boundary conditions

The configuration under study corresponds to that experimentally investigated by Pfadler et al. [17, 18] who carried out experiments with a rod stabilized flame at atmospheric pressure. Here, perfectly premixed fuel and air are supplied to 48 mm diameter tube, where 10 mm above the exit a 1.6 mm rod is situated for flame stabilisation. A 150 mm diameter coflow with low velocity of 0.3 m/s prevents environmental influence in the measurement region. A turbulence grid with hexagonally oriented holes being situated 100 mm upstream of the exit produces nearly homogeneous turbulence conditions. The burner set up and geometry is sketched in Fig. 2.

Flame	Methane/air	Stoichiometry: 0.8
Bulk velocity	U [m/s]	3.50
Turbulent rms velocity	U'(m/s)	0.55
Reynolds number	Re [--]	10,188
Turbulent Reynolds number	Ret [--]	148
Unburnt density	[kg/m3]	1.10
Burnt density	[kg/m3]	0.17
Laminar burning velocity	S_L [m/s]	0.27

Table 1 Boundary Conditions

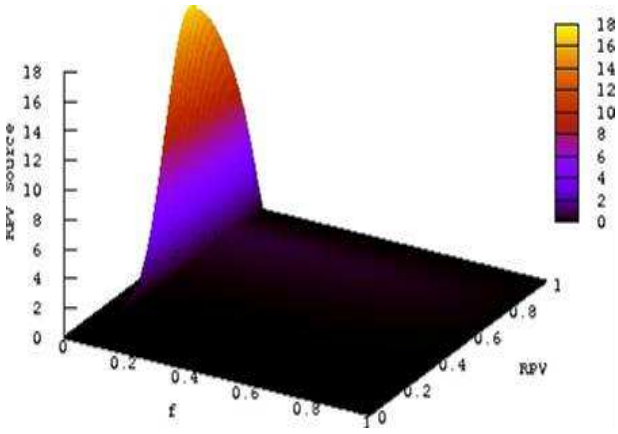

Figure 1 RPV source term in mixture fraction and normalized RPV

Two-dimensional instantaneous velocity information can be obtained with particle image velocimetry (PIV). For that the flow field is seeded with small tracer particles (TiO2, d_{mean} = 1

micro), which follow the turbulent flow adequately. Stereo PIV measurements of all three velocity components in the measurement plane were possible with two PIV cameras. For the measurement of the three-dimensional rate-of-strain tensor, a dual plane approach was used, consisting of two complete stereo PIV systems. The details of the complex system (synchronisation procedure, data storage, validation and evaluation) are described by Pfadler et al. [17, 18, 19].

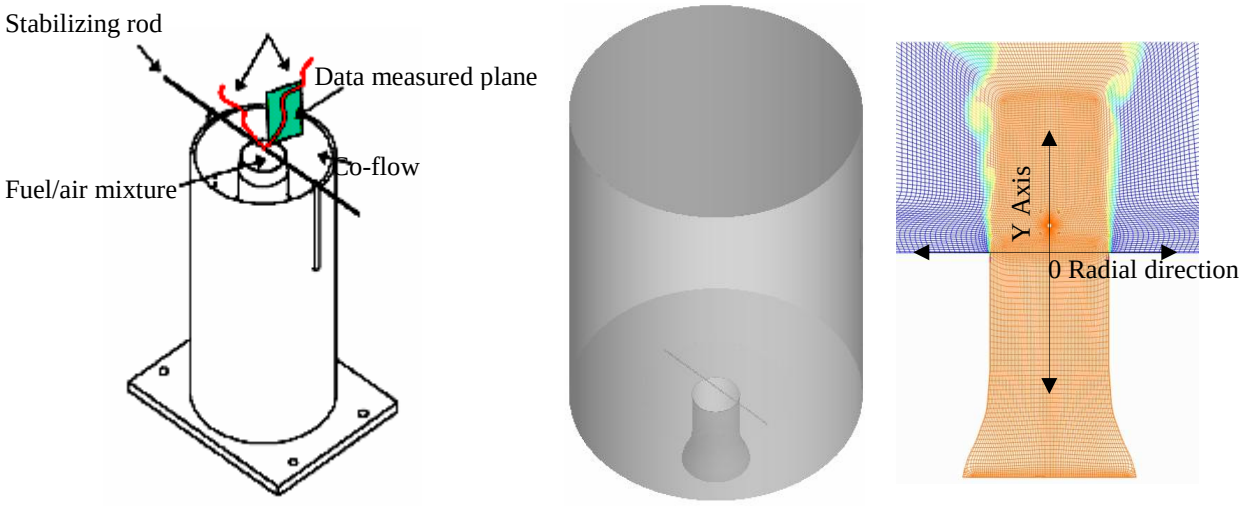

Figure 2 Burner set up(left) [19] Simulated domain with nozzle and flame stabilizing rod (middle) and representation of mesh on a plane across the stabilization rod and passing through centre line of the nozzle with super imposed by instantaneous mixture fraction(right)

The flame characterized by Reynolds numbers of 10,188 is investigated here. All the flame parameters are summarized in Table 1. For representing this geometry numerically, the turbulence grid with circularly oriented 86 holes was included in the computational domain along with the pipe (see sectional view in figure 1(bottom right))

Fig.1 Burner set up(top) [19] Simulated domain with nozzle and flame stabilizing rod (bottom left) and representation of mesh on a plane across the stabilization rod and passing through centre line of the nozzle with super imposed by instantaneous mixture fraction(bottom right)

This consists of 206 structured blocks featuring an O-type structure. The total amount of grid points on the fine grid is 1.3 millions. The block structured mesh was constructed with ICEMCFD and elliptical smoothening is carried out on it for getting better convergence. All simulations were run on 8 processors. The domain is extended with coarse mesh radially beyond co-flow region to accommodate numerical instabilities due to the limitations of availability of pressure boundary conditions at outlet.

As inlet boundary conditions, the mass flows from the experiment were prescribed using laminar unperturbed profiles. A laminar inlet profile is sufficient for such a simulation since the flow field is dominated by the intense shear of the jets produced by the turbulent grid at upstream. The co-flow air stream was assumed to be homogeneous. Again, a constant mean value was prescribed for the velocity of 0.3 m/s. Thickness of 1mm for the nozzle separating the fuel jet and the co-flow is considered as in experiments. Mixture fraction of fuel at fuel

inlet is specified as 0.0445, which corresponds to the premixed methane fuel (stoichiometry of 0.8), and for co-flow as zero. Outlet boundary at top is given as convective boundary and other regions with open boundaries are given as slip wall with zero velocity.

All the governing equations are integrated into a three dimensional finite-volume in house FSASTEST-3D CFD code. The code features geometry-flexible block-structured, boundary-fitted grids with a collocated, cell-centered variable storage. Second-order central schemes are used for spatial discretization except for the convective term in the scalar transport equation. Here, a flux-limiter with TVD (total variation diminishing) properties is employed to ensure bounded solutions for the mixture fraction [13, 14]. Pressure-velocity coupling is achieved via a SIMPLE similar procedure extended for low-Mach flows. For the time stepping multiple stage Runge-Kutta schemes (here: three stages) with second order accuracy are used. Following a fractional step formulation, in each stage a momentum correction is carried out in order to satisfy the continuity. The code is parallelized based on domain decomposition using the MPI message passing library.

Results and Discussions

Three different types SGS scalar flux models are investigated on the V-Flame methane-air premixed combustion configuration. Results obtained from three different models are analyzed and compared against experimental data available. First insight on the capability of models under consideration in predicting the flow field is demonstrated, before discussing the combustion and SGS scalar flux fields' predictability. Radial profiles of velocity are available only at one location in the domain at 2 mm downstream from the exit of the nozzle. The radial velocity profiles of mean axial and mean radial velocities are compared against the experimental data in Fig. 3. All models could able to capture the experimental data well. Radial velocity profiles of mean axial, mean radial velocities and their fluctuations obtained from three models are compared against each other at 0.012 m (just above the v-flame stabilization rod), 0.05 m and 0.1 m downstream locations from the exit of nozzle in Fig. 4 and Fig 5. The newly implemented SGS scalar flux models doesn't influence the flow field directly, though it can alter flow field due to the density dependency. In Fig. 4(left-bottom), axial velocities at 0.012 mm from the exit of nozzle in the downstream plotted show that stagnation zone above the rod is formed, which is crucial for flame stabilization. Stagnation zone formed above the rod is very thin and it is in the order of a one millimeter. All three models could capture well this stagnation zone. The temperature of the heated flame stabilization rod is not important in stabilizing the flame. To capture well these phenomenon total 25 nodes were placed on the circumference of the flame stabilization rod. Stagnation zone in the downstream at y = 0.05 m (left-middle) and at y = 0.1 m (left-top) are disappeared. Though all models are predicting axial velocities in agreement with other models, anisotropic model estimated the slower disappearance of stagnation zone at y=0.05 over others'. From fig 4.(Left-top) it is evident that the fuel jet started spreading out at y=0.1 m. Axial velocity fluctuations are shown in Fig 4(right). In all three locations two main peaks are observed. One is at shear layer between the fuel jet and co-flow and other one is in

flame front. In other locations axial velocity fluctuations are small. It also observed that shear layer and flame front are very close to each other at y=0.1 m. Magnitude of axial velocity fluctuations are found to increasing along the downstream from y=0.012 to y=0.05 m. All three models are predicting axial velocity and it fluctuations very similarly.

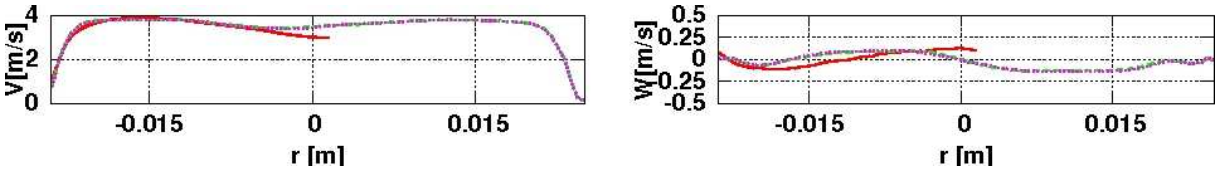

Figure 3 Time averaged mean axial (left) radial (right) velocity Experimental (—), EDM (…), Dynamic EDM (…), Anisotropic (…) at y=0.002 m

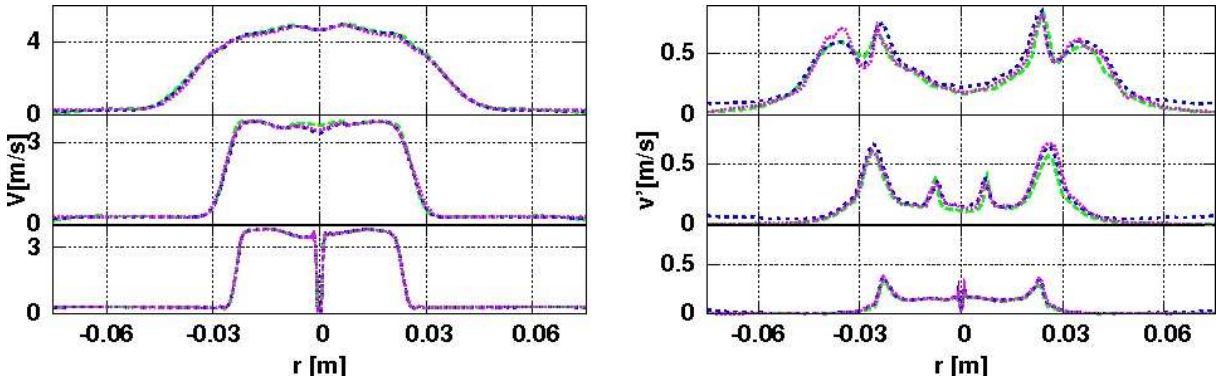

Figure 4 Time averages mean axial velocity (left) fluctuations (right) EDM (…), Dynamic EDM (…), Anisotropic (…) at y=0.012 m (bottom), y=0.05 m(middle), y=0.1 m (top)

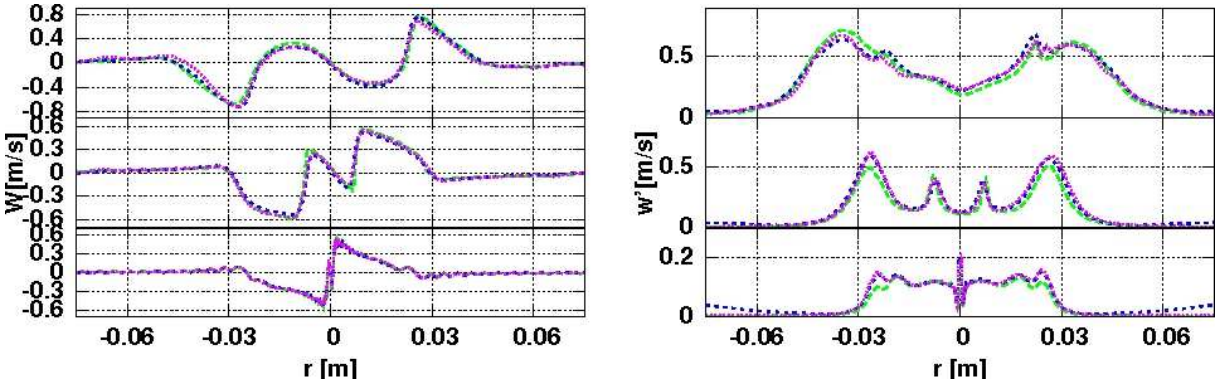

Figure 5 Time averages mean radial velocity (left) fluctuations (right) EDM (…), Dynamic EDM (…), Anisotropic (…) at y=0.012 m (bottom), y=0.05 m(middle), y=0.1 m (top)

Radial velocities and its fluctuations are having similar behavior like axial velocity component. Maximum radial velocity in flame zone is found at centre in upstream region and is moving away from centre in downstream. Non-zero radial velocities are found at radial distance greater than co-flow radius at y=0.1 m predicting the spread of fuel jet radially. Though all three models are predicting similar profiles, predictions from EDM are different with other two models marginally. Radial velocity fluctuations from the eddy diffusivity are different other two models. These can also influence on the flame thickness and will be discussed in the later part of results.

In the experiments temperature measured as the progress variable and in FGM based approaches the RPV is based on the concentration of specie(s). Temperatures and other species (like CO, OH, CO2 and etc) concentrations are obtained as only a post process variable from beta integrated FGM table rather than a transported quantities. The detailed experimental data in the experimental measured area (EMA) is available on one side of the V-flame, reaching from the axis to a radius of 17 mm and in height from 4.5 to 22.5 mm above the stabilization rod. The time averaged reaction progress variable based on temperature in both experiment and simulations plotted in Fig 6 shows the well predictability of the model used. Here it is worth mentioning that the flame front from Fig.2 is away from the mixing zone (in Fig.2 (right)) between co-flow and main fuel jet, which clearly points out that the co-flow is not influencing the flame behaviour in the vicinity of the stabilization rod. Iso-surfaces of instantaneous temperature gradient shown in Fig.7 (right) clearly predict that the flame is stabilized on the rod and the V-shape of the flame is recovered well. It shows in addition the highly turbulent nature of the flame front. The instantaneous RPV source term, which is being used in simulations are plotted in Fig.7 (left), outlines the reaction zone of the flame. This reaction zone is very thin which makes the combustion modelling very challenging as the fuel is transformed completely from burnt to un-burnt within a control volume. So, it may be very interesting to see the models for the sub-grid scales in detail as discussed later in this section.

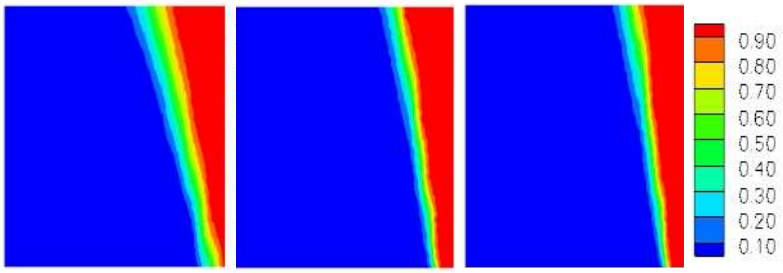

Figure 6 RPV Experiment (left), Eddy diffusivity Model (middle), anisotropic model

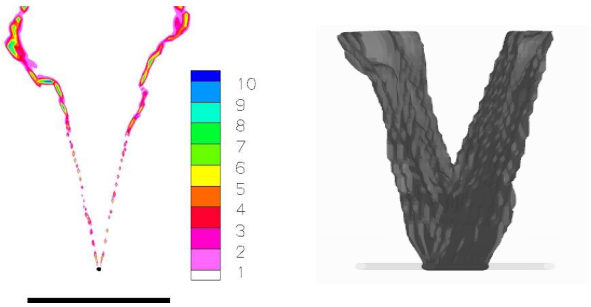

Figure 7 Reaction progress variable source term (left) and Temperature gradient

To get further overview of the model capability and more insights into the predictions radial profiles of mean combustion properties such as temperature, temperature fluctuations, reaction source and reaction source fluctuation are plotted in Fig 8 and Fig. 9. Temperature profiles locate the flame position. Fig. 8 shows the thickness of the temperature profile getting thicker along the downstream of the domain, which characterises the V flame shape. Maximum temperature for this configuration is about 2000 K. The temperature is suddenly

jumping from inlet fuel jet temperature to the adiabatic flame temperature in about 1 mm as seen in Fig 8(left). All three models here under investigation predicting the flame location similar, new models proposed here estimated blunt jump rather than sharp jump as in the EDM. Experimental investigation showed that flame brush is thicker, which better captured by the both new models. This gives an indicating the dynamic diffusion coefficient is playing an important role in determining the flame front more exactly. Time Averaged Temperature Fluctuations are plotted in Fig 8(right) shows trend of the radial profiles at all three locations are same and they alike. Time averaged is as high as 600 K and they are thicker, which indicates the flame fluctuating in space especially more in downstream. Temperature fluctuation predictions from new model are higher and wider than that of the EDM.

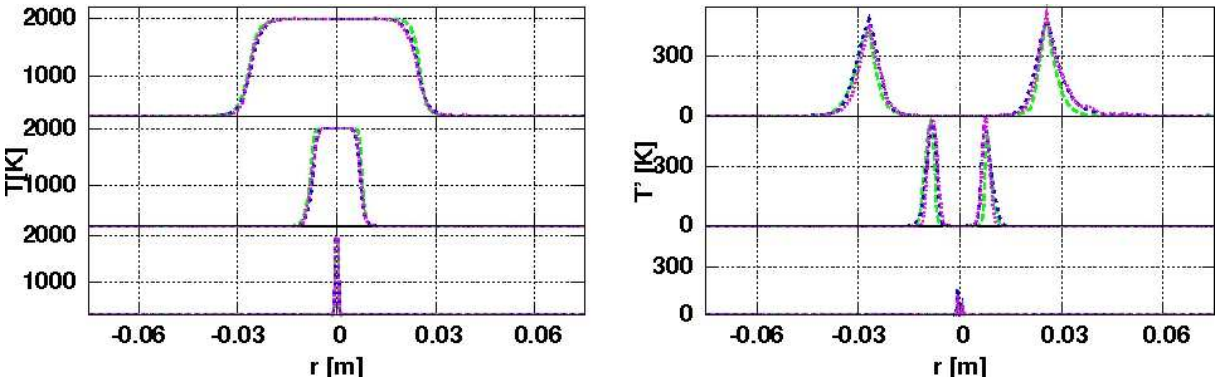

Figure 8 Time averages mean radial temperature (left) fluctuations (right) EDM (…), Dynamic EDM (…), Anisotropic (…) at y=0.012 m (bottom), y=0.05 m(middle), y=0.1 m (top)

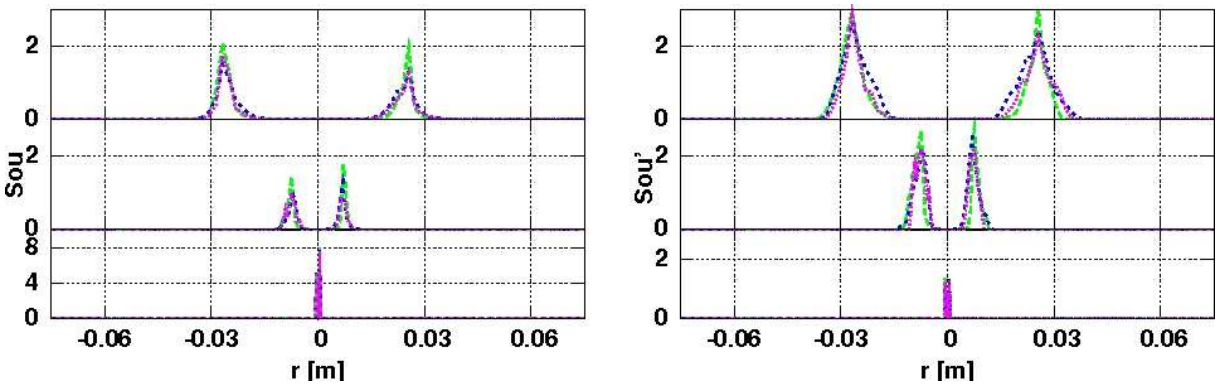

Figure 9 Time averages mean radial RPV source (left) fluctuations (right) EDM (…), Dynamic EDM (…), Anisotropic (…) at y=0.012 m (bottom), y=0.05 m(middle), y=0.1 m (top)

SGS fluxes in the EMA region are plotted in Fig. 10. For an easier interpretation of the results, let us mention that FGM model solves absolute reaction progress variable whereas experimental data is available as normalized temperature based RPV. To bring similarity between them RPV from simulations are normalized based on equilibrium value corresponding to mixture fraction values. Since the reaction zone is very thin in this configuration and Lewis number is unity for the fuel under investigation, it can be assumed that both RPV from experiments and simulations are comparable, and an assessment of the model capability is thus possible. RPV source terms and their fluctuations plotted in Fig 9 show that EDM predicts higher values than Dynamic EDM and Anisotropic models.

To assess further the investigated classical eddy viscosity SGS scalar flux model against new anisotropic model, a comparison of the axial and radial scalar fluxes of RPV are carried out against the experimental data. The SGS flux change in physical co-ordinates may not able give the more insight as the flame is changing from burnt to unburnt in a single cell. To overcome this difficulty in understanding the model capability, SGS scalar fluxes in EMA region are plotted in the normalized reaction progress variable space which represents the flame brush.. Where as the SGS fluxes in the flame brush are having better range of variation. Classical Eddy Diffusivity Model (EDM) predicts the higher magnitude SGS scalar fluxes near unburnt location, where as Anisotropic model predicts the higher magnitude of SGS fluxes in the middle of flame brush as in experiments. EDM of SGS scalar flux is not able predict the both the trend and magnitude of the experimental findings. Though anisotropic model couldn't capture magnitude of the SGS scalar flux accurately, trends are captured well in mixture normalized progress variable space. These observations substantiate the argument that the thickness of the flame is influenced by sub grid scale fluxes, and it is very much important especially in the context of premixed combustion and variable turbulent Schmidt number to concentrate on this aspect.

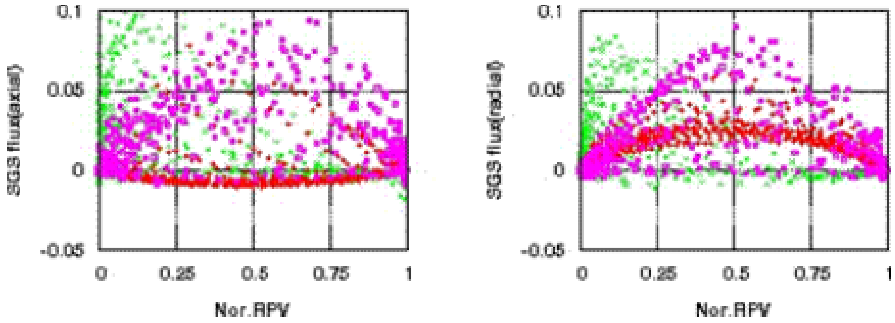

Figure 10 RPV SGS scalar flux axial (left) and radial (right) in normalized RPV space Experimental (red), EDM(green), Anisotropic (pink)

Conclusions

The ability of combustion-LES to correctly describe turbulent premixed combustion has been appraised on a rod stabilized unconfined flame. The technique combines the flamelet generated manifold (FGM)-tabulated chemistry approach with LES and accounts for the variable local equivalence ratio due to a possible entrainment of the environment air through a mixture fraction variable LES results of the rod stabilized flame compared satisfactory with experimental data for the flow field quantities and species concentrations. Dynamic EDM and newly proposed Different SGS scalar flux models predicted flow fields quantities consisting with each other. Dynamic EDM and Anisotropic model are able to capture flame brush thickens more accurately than classical EDM model.

Acknowledgements

For financial support we gratefully acknowledge the DFG (German Research Foundation).

References

[1] Janicka J., and Sadiki. A., 2004, Proc. Combust. Institute, 30: 537-547.

[2] Pitsch, H. (2006), Large Eddy Simulation of Turbulent Combustion, Ann. Rev. Fluid Mech., (38) (2006), pp. 453–482.

[3] Warnatz, J., Maas U., and Dibble RW. (1996) Combustion, Springer Verlag.

[4] Pope. S.B. (2000), Turbulent Flows. Cambridge Universtiy Press, Cambridge

[5] J.A. van Oijen, L.P.H. de Goey, A numerical study of confined triple flames using a flamelet-generated manifold, Combust. Theory Modelling, 8(1), 141-163, (2004)

[6] van Oijen, J.A., Bastiaans, R.J.M., and L.P.H. de Goey, L.P.H., (2007) Low-dimensional manifolds in direct numerical simulations of premixed flames Proc. Combust Inst., 31 (2), pp. 1377–1384.

[7] D. Veynante, J. Piana, J.M. Duclos, C. Martel, Experimental analysis of flame surface density models for premixed turbulent combustion, Symposium (International) on Combustion, Volume 26, Issue 1, 1996, Pages 413-420

[8] Pascale Domingo, Luc Vervisch, Sandra Payet, Raphael Hauguel, DNS of a premixed turbulent V flame and LES of a ducted flame using a FSD-PDF subgrid scale closure with FPI-tabulated chemistry, Combustion and Flame, Volume 143, Issue 4

[9] Bell, J. B., Day, M. S., Shepherd, I. G., Johnson, M. R., Cheng, R. K., Grcar, J. F., Beckner, V. E., and Lijewski, M. J., Numerical simulation of a laboratoryscale turbulent V-flame. PNAS, 2005. 102(29): p. 10006-10011.

[10] B. Manickam, S. P. R. Muppala, J. Franke, and F. Dinkelacker Numerical simulation of rod stabilized flames Lisbon, ECCOMAS CFD 2010, Portugal, 14–17 June 2010

[11] Germano M., Piomelli U., Moin P., and Cabot W. H., 1991, Phys. Fluids A, 3: 1760-1765.

[12] Sagaut, P., (2001), Large Eddy Simulation for incompressible Flows, Springer, Berlin, 2001

[13] Wegner, B. Maltsev, A., Schneider, C., Sadiki, A., Dreizler, A., Janicka, J. (2004), Assessment of unsteady RANS in predicting swirl flow instability based on LES and Experiments. International Journal of Heat and Fluid Flow, 25:528-536, 2004.

[14] Wegner, B. (2007), A Large-Eddy Simulation Technique for the Prediction of Flow, Mixing and Combustion in Gas Turbine Combustors. PhD thesis, Technische Universit¨at Darmstadt.

[15] Huai, Y., Sadiki, A.: Analysis and optimization of turbulent mixing with large eddy simulation. In: ASME 2nd Joint U.S.-European Fluids Engineering Summer Meeting, FEDSM 2006-98416, Miami (2006)

[16] Landenfeld, T. Sadiki, A. Janicka, J. A Turbulence-Chemistry Interaction Model Based on a Multivariate Presumed Beta-PDF Method for Turbulent Flames,Flow, Turbulence and Combustion, Volume 68,Issue 2, pp 111-135,2002

[17] Pfadler, J. Kerl, F. Beyrau, A. Leipertz, A. Sadiki, J. Scheuerlein, F. Dinkelacker, Direct evaluation of the subgrid-scale scalar flux in turbulent premixed flames with conditioned dual-

[18] S. Pfadler, F. Dinkelacker, F. Beyrau, A. Leipertz, High resolution dual-plane stereo-PIV for validation of subgrid scale models in large-eddy simulations of turbulent premixed flames, Combustion and Flame, 156, 1552-1564 (2009).

[19] Sebastian Pfadler, Frank Beyrau, and Alfred Leipertz, "Flame front detection and characterization using conditioned particle image velocimetry (CPIV)," Opt. Express 15, 15444-15456 (2007)

[20] Ketelheun, A. : Olbricht, C. : Hahn, F. : Janicka, J. , Premixed Generated Manifolds for the Computation of Technical Combustion Systems. In: ASME Turbo Expo, Orlando, Florida, USA (GT2009-59940)

[21] Sadiki, A., Huai, Y.: Assessment of an Explicit Anisotropy-resolving Algebraic ScalarFlux SGS Model for LES of Turbulent Mixing Processes. Int. J. Heat and Fluid Flow (submitted)

[22] Cabot , W. , Moin, P, " Large Eddy Simulations of Scalar Transport with the Dynamic Subgrid-Scale Model", Large Eddy Simulation of Complex Engineering and Geophysical Flows" , 1993, Cambridge University Press

[23] Pantangi, P., Huai, Y., Sadiki, A., Mixing Analysis and Optimization in Jet Mixer Systems by Means of Large Eddy Simulations, In Micro and Macro Mixing: Analysis, Simulation and Numerical Calculation (Eds.: Bockhorn, Mewes, Peukert, Warnecke), Heat and Mass Transfer Series, p. 205-226, 201

[24] Sadiki, A. "Extended Thermodynamics as Modeling Tool of Turbulence in Fluid Flows" Trends in Applications of Mathematics to Mechanics, Shaker Verlag, Aachen,pp. 451-462, (2005)

[25] Y. Huai, K. Björg, A. Sadiki, S. Jakirlic, " Large Eddy Simulations of Passive-scalar Mixing using a New Tensorial Eddy Diffusivity based SGS-Modeling", European Turbulence Conference, Portugal, 200Y. Huai, "Large Eddy Simulation in the Scalar field", Doctoral thesis,TU Darmstadt 2005

[26] J. Andreopoulos, W.Rodi, "Experimental investigation of jets in a cross flow", J. Fluid Mech., Vol.138, pp.93–127, 1984